Journal of Organometallic Chemistry, 394 (1990) 213–233
Elsevier Sequoia S.A., Lausanne
JOM 20868

Oxygen tripod ligand supported molybdenum and tungsten carbyne complexes: carbon–carbon bond formation reactions. Crystal structures of $[L(CO)_2W{\equiv}CC_6H_4\text{-}p\text{-}CH_3]$ and $[L(CO)\overline{Mo(\mu\text{-}CO)\underline{Pd(I)C}}\underline{(C_6H_4\text{-}p\text{-}CH_3)C_6H_4\text{-}o\text{-}CH_2N}(CH_3)_2]$, $L^- = [(C_5H_5)Co\{P(O)(OCH_3)_2\}_3]^-$ *

Wolfgang Kläui *, Harry Hamers

Institut für Anorganische Chemie der Technischen Hochschule Aachen, Templergraben 55,
D-5100 Aachen (F.R.G.)

Michel Pfeffer *,[1], André de Cian [2] and Jean Fischer [2]

[1] Laboratoire de chimie de coordination, URA 416 du CNRS, and [2] Laboratoire de cristallochimie
et de chimie structurale, URA 425 du CNRS, Université Louis Pasteur, 4 rue Blaise Pascal
F-67070 Strasbourg Cédex (France)

(Received February 16th, 1990)

Abstract

Several carbyne complexes of the type $[L_R(CO)_2M{\equiv}CC_6H_4\text{-}p\text{-}CH_3]$ (**1**) (where L_R^- is the tris-chelating oxygen ligand: $[(C_5H_5)Co\{P(O)R_2\}_3]^-$, R = OMe, OEt, O-i-Pr; M = Mo, W) have been synthesized. One of these, $[L_{OMe}(CO)_2W{\equiv}CC_6H_4\text{-}p\text{-}CH_3]$ (**1a**) was fully characterized by a crystal structure determination. Complex **1a** adds one mole of trimethylphosphine to afford high yields of a tungstacyclopropenone derivative, $[L_{OMe}(CO)\{P(CH_3)_3\}W(\eta^2\text{-}C(O)CC_6H_4\text{-}p\text{-}CH_3)]$ (**2**), which is formed via formal migration of CO to the M≡C bond. On the other hand, the molybdenum complexes **1c–e** [R = OMe (**1c**), OEt (**1d**), O-i-Pr (**1e**)] react with trimethylphosphine exclusively by CO displacement to afford $[L_R(CO)\{P(CH_3)_3\}\text{-}Mo{\equiv}CC_6H_4\text{-}p\text{-}CH_3]$ (**3a–c**). The reaction requires several days at room temperature to reach completion, and no intermediates (e.g. of type **2**) are detected. When the carbyne complexes **1a** and **1c** react with di-μ-iodo-bis(*N*,*N*-dimethylaminomethylphenyl-2*C*,*N*)dipalladium, $[\{(dmba)PdI\}_2]$, insertion of the M≡C bond into the Pd–C bond takes place. Only one regioisomer, namely the carbon–carbon coupling product, $[L_{OMe}(CO)\overline{M(\mu\text{-}CO)\underline{Pd(I)C}}\underline{(C_6H_4\text{-}p\text{-}CH_3)C_6H_4\text{-}o\text{-}CH_2N}(CH_3)_2]$

---

* Dedicated to Professor F.G.A. Stone on the occasion of his 65th birthday, with the grateful thanks of one of us (M.P.) for a fruitful post-doctoral stay in Bristol, where he learned a lot of organometallic chemistry and much else.

[M = W (**4a**), Mo (**4b**)] was observed. The crystal structure of **4b** was determined. The carbyne carbon atom of **1c** is σ-bonded to the *ortho* carbon of the dmba moiety and the palladium atom interacts strongly with this carbon atom, the molybdenum center, and a CO group. The new organometallic ligand can be regarded as a unprecedented metalla-allyl unit η^3-bonded to palladium. The ^1H and ^{31}P NMR spectra of the compounds have been analyzed.

Introduction

Metal carbyne complexes have attracted the attention of many chemists since the discovery of such compounds by E.O. Fischer and his group in 1973 [1]. The reactivity of the metal–carbon triple bond in carbyne complexes [2] has been studied by several groups with the aim of using the carbyne fragment as building block in organic synthesis or utilizing the metal–carbon triple bond as a sterically hindered hetero-acetylene, e.g. in cluster synthesis [3,4]. We recently prepared the first molybdenum and tungsten carbyne complexes of the type $[L_R(CO)_2M{\equiv}CAr]$ [5], where L_R^- denotes anionic tridentate oxygen ligands of the type $[(C_5H_5)Co\{P(O)R_2\}_3]^-$. The $6e^-$-ligands L_R^- are formally equivalent to the $6e^-$-cyclopentadienyl ligand, but have electronic properties like those of fluoride or oxide ligands. We describe below the synthesis of a series of $[L_R(CO)_2M{\equiv}CAr]$ compounds and the first crystal structure determination of such a carbyne complex, which confirms the molecular structure proposed previously on the basis of spectroscopic data. Insertion of alkynes into the Pd–C bond of cyclopalladated compounds has attracted our attention for several years now, since these reactions either give novel organopalladium compounds or provide new routes to heterocyclic organic products [6]. We therefore thought it of interest to compare the reactivity of metal–carbon triple bonds with that of carbon–carbon triple bonds toward compounds with a palladium-carbon bond. The complexes $[L_R(CO)_2M{\equiv}C\text{-}Ar]$ (**1**) were thought to be a good choice for this comparison, since the anionic tridentate ligands L_R^- have a pronounced stabilizing effect on the $[(CO)_2M{\equiv}CAr]^+$ fragment [5] and this could prevent decomposition of the starting material prior to reaction.

Preparative results and discussion

The molybdenum and tungsten carbyne complexes $[L_R(CO)_2M{\equiv}CC_6H_4\text{-}p\text{-}CH_3]$ (**1**) are accessible from *trans*-$Br(CO)_4M{\equiv}CC_6H_4\text{-}p\text{-}CH_3$ and NaL_R, the sodium salts of the oxygen ligands (see Scheme 1). They can all be handled in air and exhibit high thermal stability, like the analogous carbyne complexes which we recently described [5]. Their reaction with trimethylphosphine leads to different products, depending on the metal M (molybdenum or tungsten). The addition of trimethylphosphine to the tungsten compound $[L_{OMe}(CO)_2W{\equiv}CC_6H_4\text{-}p\text{-}CH_3]$ (**1a**) induces coupling of the carbyne with a carbonyl carbon to give the η^2-ketenyl complex $[L_{OMe}(CO)\{P(CH_3)\}W(\eta^2\text{-}C(O)CC_6H_4\text{-}p\text{-}CH_3)]$ (**2**). The reaction of trimethylphosphine with the molybdenum compounds **1** [R = OMe (**1c**), OEt (**1d**), and O-i-Pr (**1e**)] yields the CO-substitution products $[L_R(CO)\{P(CH_3)_3\}Mo{\equiv}CC_6H_4\text{-}p\text{-}CH_3]$ (**3a–c**), exclusively. Both the ketenyl complex **2** and the compounds of type **3** are red-violet and soluble in polar organic solvents. The carbyne complexes **3** are also

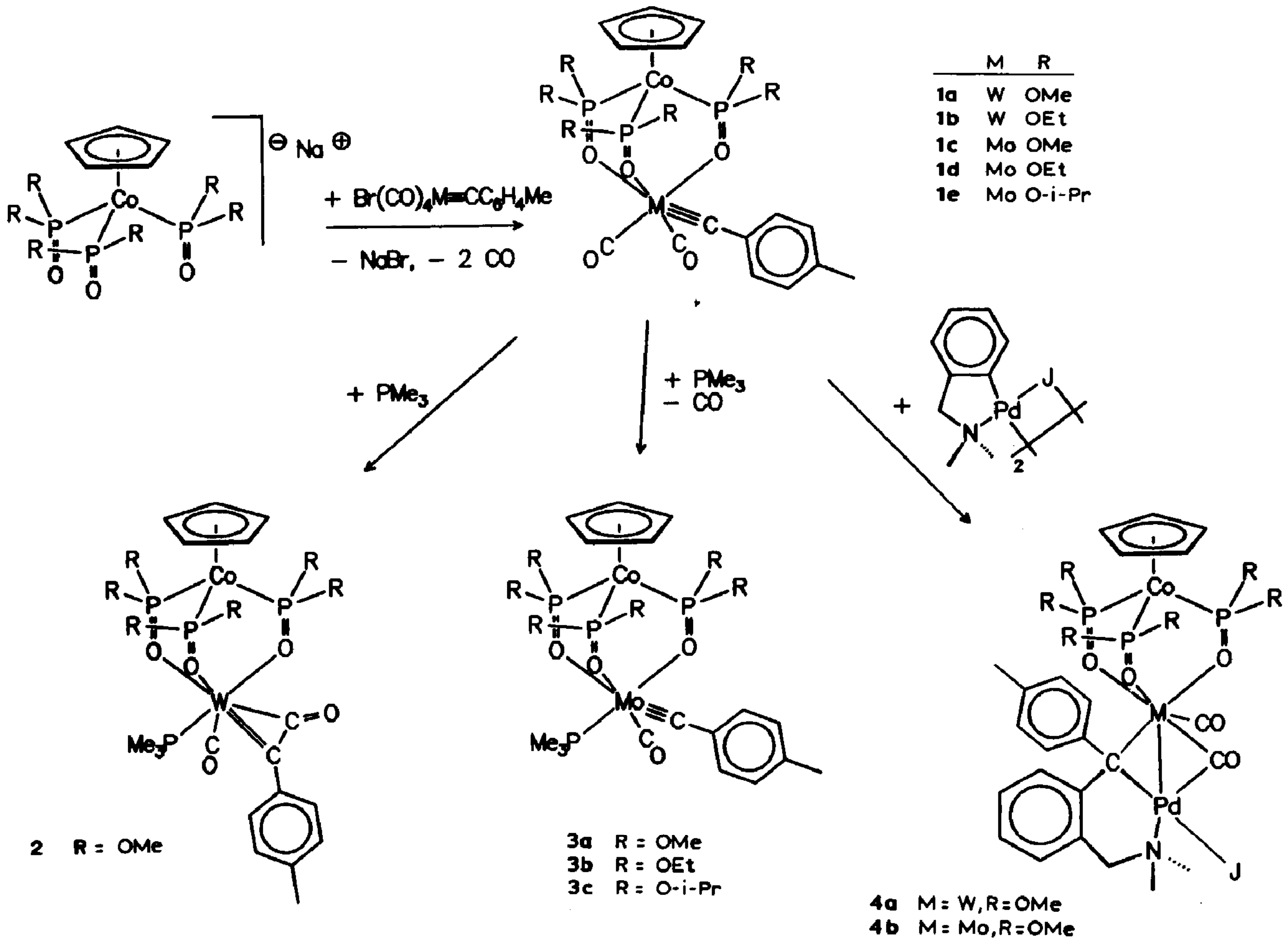

	M	R
1a	W	OMe
1b	W	OEt
1c	Mo	OMe
1d	Mo	OEt
1e	Mo	O-i-Pr

Scheme 1.

soluble in saturated hydrocarbon solvents. The proposed structure of **2**, with a ketenyl unit η^2-bonded to W (which would also be described as a tungstacyclopropenone derivative), is based on the IR and NMR data (see below), which agree well with those of related compounds synthesized by Kreissl et al. and characterized by a crystal structure determination [7a–c]. Whether the coordination of trimethylphosphine at the tungsten center and the carbon–carbon bond formation occur in a concerted process, or intermediate decoordination of one oxygen donor center of the tripod ligand takes place, is a matter for further investigation. The CO-substitution reaction leading to the molybdenum compounds **3a–c** requires several days (3–4) to go to completion, and no intermediates could be detected from the IR spectra. This is in contrast with the results reported by Kreissl et al. [7], who observed several types of compounds when trimethylphosphine was added to the corresponding cyclopentadienyl complexes $[(C_5H_5)(CO)_2M{\equiv}CR]$, namely η^1,η^2-ketenyl complexes and products of CO displacement. This illustrates both the lower reactivity and the higher selectivity of the carbyne unit stabilized by the oxygen ligand compared with those of the cyclopentadienyl analogue.

Carbon–carbon triple bonds insert into the palladium–carbon bond of di-μ-iodo-bis(*N*,*N*-dimethylaminomethylphenyl-2*C*,*N*)dipalladium $[\{(dmba)PdI\}_2]$ [6a] to yield seven- and nine-membered rings. The metal–carbon triple bond of $[L_{OMe}(CO)_2M{\equiv}CC_6H_4\text{-}p\text{-}CH_3]$ [M = W (**1a**), Mo (**1c**)] reacts with the palladium complex $[\{(dmba)PdI\}_2]$ at room temperature in dichloromethane to give the insertion products $[L_{OMe}(CO)\overline{M(\mu\text{-}CO)\underline{Pd(I)}C}\underline{(C_6H_4\text{-}p\text{-}CH_3)C_6H_4\text{-}o\text{-}CH_2N}(CH_3)_2]$ (**4a,b**, see Scheme 1) which were isolated as black-brown needles. The products are stable for some time in the solid state under dry nitrogen at low temperature but decompose readily in solution in the presence of light to deposit a palladium mirror. The crystal structure determination of compound **4b** (see below) shows that the carbyne carbon atom C12 is sigma-bonded to the *ortho* carbon of the dmba unit. There are also close contacts between the palladium atom and C12, the molybdenum atom, and one CO group. The geometry around palladium is that of a distorted square plane. In order to achieve a 16-electron configuration for the palladium center, it has to be assumed that C12, molybdenum, and the bridging CO group contribute four electrons to the electron count. Thus this part of the molecule can be regarded as a metalla-allyl unit η^3-bonded to the Pd atom.

The insertion of the metal–carbon triple bond could have taken place in two different orientations. We detected only that shown in Scheme 1. The regioselectivity is the opposite of that found when studying the insertion of asymmetric alkynes into the Pd–C bond of cyclopalladated compounds. The carbon–carbon triple bond is always inserted with an orientation such that the carbon atom linked to palladium bears the less bulky group [6,8], whereas in **4a,b** the more bulky group $LM(CO)_2$ is linked to palladium.

Crystal structure of $[L_{OMe}(CO)_2W{\equiv}CC_6H_4\text{-}p\text{-}CH_3]$ (1a)

The structure of the carbyne complex $[L_{OMe}(CO)_2W{\equiv}CC_6H_4\text{-}p\text{-}CH_3]$ (**1a**) together with the atom numbering scheme is shown in Fig. 1. The main distances and angles are listed in Table 2, and the positional parameters in Table 1.

The carbyne complex $[L_{OMe}(CO)_2W{\equiv}CC_6H_4\text{-}p\text{-}CH_3]$ (**1a**) has the structure expected for a compound of the type $[(6e^-\text{-ligand})(CO)_2W{\equiv}CR]$. An ORTEP drawing is

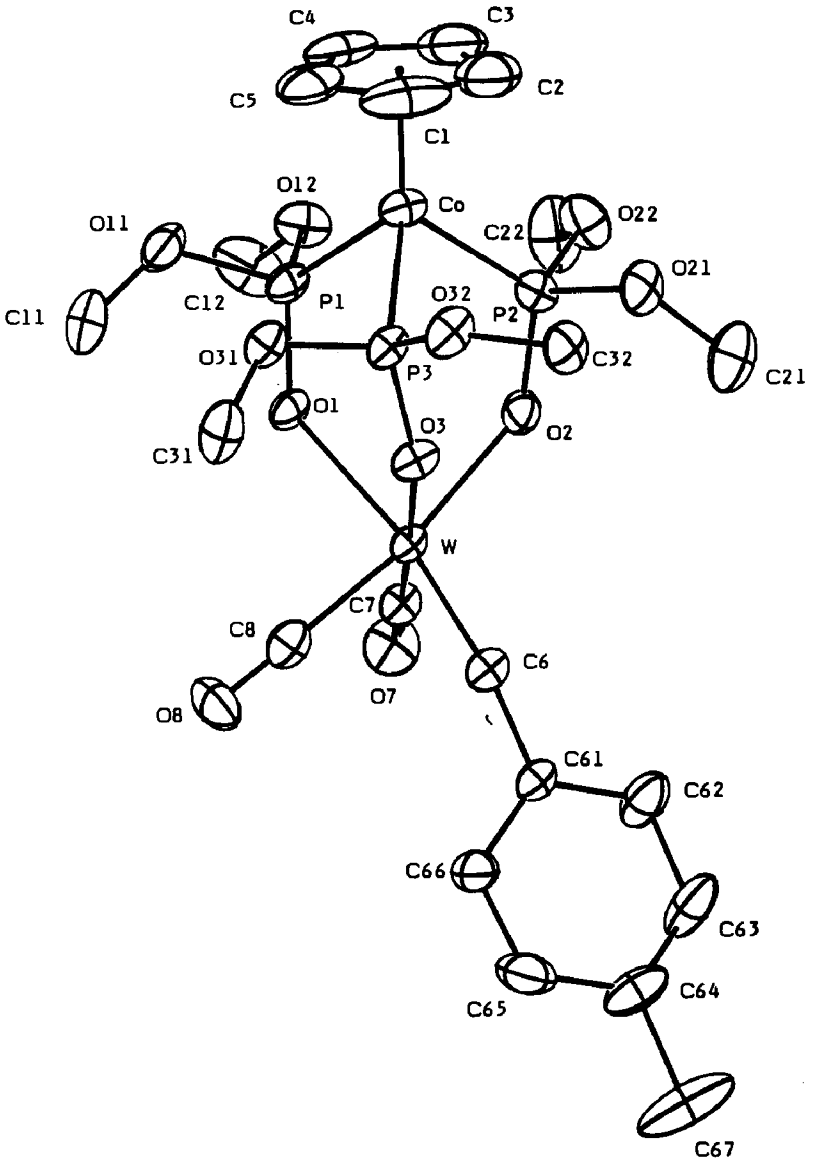

Fig. 1. ORTEP drawing [9] of the molecular structure of [$L_{OMe}(CO)_2W{\equiv}CC_6H_4$-*p*-$CH_3$] (**1a**). Non-hydrogen atoms are shown as 10% thermal ellipsoids. H-atoms are omitted for clarity.

presented in Fig. 1. The tungsten atom possesses octahedral coordination geometry and the idealized symmetry of the molecule is C_S.

The tripod ligand L_{OMe}^- occupies three facial positions of the octahedron formed by the atoms O1, O2, O3, C6, C7, C8. The other three positions are occupied by the three carbon atoms of the carbon monoxide ligands and the carbyne unit. The octahedron is *trigonally elongated* along the tungsten-cobalt axis. The O–W–O angles of the P=O oxygen atoms and the C–W–C angles of carbon atoms C6, C7, and C8 are ca. 82°.

The short tungsten–carbyne carbon distance of 1.803(6) Å is in accord with the formulation as metal–carbon triple bond. This bond length obviously does not vary

Table 1

Final positional parameters [a] with their estimated standard deviations for $[L_{OMe}(CO)_2W{\equiv}CC_6H_4\text{-}p\text{-}CH_3]$ (**1a**)

Atom	x	y	z	B (Å^2)
W	0.1775(3)	0.21340(2)	0.18459(2)	3.625(6)
Co	0.2954(1)	0.38942(6)	0.0943(1)	4.96(3)
P1	0.4108(2)	0.3275(1)	0.1958(2)	4.55(5)
P2	0.1318(3)	0.3717(1)	0.1779(2)	4.58(5)
P3	0.2432(2)	0.3115(1)	−0.0073(2)	4.29(5)
O1	0.3638(5)	0.2612(3)	0.2114(4)	4.5(1)
O2	0.1101(6)	0.3052(3)	0.2184(5)	5.2(1)
O3	0.1772(6)	0.2575(3)	0.0356(4)	4.7(1)
O7	0.1948(8)	0.1575(4)	0.4070(5)	7.6(2)
O8	0.3208(9)	0.0902(4)	0.1392(8)	8.9(2)
O11	0.5537(6)	0.3222(4)	0.1673(6)	7.2(2)
O12	0.4335(7)	0.3626(4)	0.3031(5)	6.1(2)
O21	0.0062(7)	0.3934(4)	0.1062(5)	6.3(2)
O22	0.1209(8)	0.4190(4)	0.2717(6)	7.2(2)
O31	0.3703(6)	0.2888(3)	−0.0525(5)	5.5(2)
O32	0.1629(7)	0.3306(4)	−0.1133(5)	6.0(2)
C1	0.314(2)	0.4474(6)	−0.0292(9)	11.6(4)
C2	0.244(2)	0.4760(7)	0.043(2)	11.7(5)
C3	0.308(2)	0.4855(6)	0.125(1)	10.8(5)
C4	0.428(1)	0.4611(5)	0.122(1)	9.3(3)
C5	0.433(1)	0.4363(6)	0.025(1)	10.4(4)
C6	0.0408(8)	0.1617(5)	0.1677(6)	4.4(2)
C7	0.1871(9)	0.1809(5)	0.3249(8)	5.1(2)
C8	0.2674(9)	0.1361(6)	0.1559(7)	5.6(2)
C11	0.602(1)	0.2675(7)	0.126(1)	8.1(4)
C12	0.491(2)	0.3306(6)	0.3942(8)	9.5(4)
C21	−0.115(1)	0.3747(8)	0.1294(9)	8.9(4)
C22	0.166(1)	0.4075(8)	0.3775(8)	9.9(4)
C31	0.375(1)	0.2334(7)	−0.114(1)	8.1(4)
C32	0.030(1)	0.3449(6)	−0.1208(8)	6.2(3)
C61	−0.0554(8)	0.1122(5)	0.1587(6)	4.4(2)
C62	−0.177(1)	0.1234(7)	0.182(1)	8.3(3)
C63	−0.270(1)	0.0762(7)	0.167(1)	9.4(4)
C64	−0.247(1)	0.0200(6)	0.1356(8)	7.8(3)
C65	−0.124(1)	0.0075(6)	0.114(1)	9.3(4)
C66	−0.028(1)	0.0519(6)	0.127(1)	7.9(3)
C67	−0.347(1)	−0.0311(8)	0.118(1)	15.0(5)

[a] Anisotropically refined atoms are given in the form of the isotropic equivalent thermal parameter defined as $(4/3)[a^2B(1,1)+b^2B(2,2)+c^2B(3,3)+ac(\cos\beta)B(1,3)]$.

significantly when L_{OMe}^- is replaced by other anionic 6e$^-$-ligands such as $C_5H_5^-$ [10], $B(pz)_4^-$ [11], or $C_2B_9H_9Me_2^{2-}$ [12] in compounds of the type $[(6e^-\text{-ligand})(CO)_2W{\equiv}CC_6H_4\text{-}p\text{-}CH_3]$. The angle W–C–C at the carbyne carbon atom is 171.1(5)°. The small deviation from linearity is probably due to lattice forces.

The different π-acceptor properties of the CO ligands and the carbyne unit are reflected in the oxygen ligand–tungsten bond lengths. Thus the W–O2 and W–O3 bonds *trans* to the carbonyl ligands (2.154(4) and 2.127(4) Å) are shorter by 0.05 and 0.08 Å than the W–O1 bond *trans* to the carbyne unit (2.204(4) Å). The same

Table 2

Selected bond angles (deg) and bond distances (Å) with their estimated standard deviations for $[L_{OMe}(CO)_2W{\equiv}CC_6H_4\text{-}p\text{-}CH_3]$ (**1a**)

P1–Co–P2	90.82(7)	Co–P1	2.150(2)
P1–Co–P3	90.45(7)	Co–P2	2.160(2)
P2–Co–P3	90.54(6)	Co–P3	2.151(2)
Co–P1–O1	118.4(2)	P1–O1	1.507(5)
Co–P2–O2	119.2(2)	P2–O2	1.527(5)
Co–P3–O3	117.4(2)	P3–O3	1.476(4)
ct–Co–W	179.4	ct–Co	1.694
W–O1–P1	134.7(2)		
W–O2–P2	134.8(2)		
W–O3–P3	135.9(2)		
O1–W–O2	81.9(2)	W–O1	2.204(4)
O1–W–O3	82.3(1)	W–O2	2.127(4)
O2–W–O3	79.7(2)	W–O3	2.154(4)
O1–W–C6	169.9(2)		
O2–W–C8	170.3(2)		
O3–W–C7	174.3(2)		
C6–W–C7	82.4(2)	W–C6	1.803(6)
C6–W–C8	82.2(3)	W–C7	1.948(7)
C7–W–C8	84.4(3)	W–C8	1.943(8)
W–C6–C61	171.1(5)	C6–C61	1.454(8)
W–C7–O7	175.7(6)	O7–C7	1.174(7)
W–C8–O8	180.0(1)	O8–C8	1.154(9)

feature has been observed for the nitrogen ligand–tungsten bond lengths of the analogous complex $[B(pz)_4(CO)_2W{\equiv}CC_6H_4\text{-}p\text{-}CH_3]$ [13].

A Newman projection along the cobalt–tungsten axis of the carbyne complex **1a** is shown in Fig. 2. Two features are evident from this projection: (i) The center of the cyclopentadienyl ring (ct), the cobalt atom, and the molybdenum atom form a nearly perfect linear arrangement, the angle is 179.41°. (ii) The CoP_3-part is rotated relative to the WO_3-part of the $Co\text{–}(P{=}O)_3\text{–}W$ cage to give dihedral angles of 6.5°, 6.5°, and 10.7°. This kind of flexibility is typical of the ligands L_R^- and of [2.2.2]-bicyclooctane, the hydrocarbon analogue of the $Co\text{–}(P{=}O)_3\text{–}W$ frame [15]. The two enantiometric torsional isomers occur in pairs in the centrosymmetric unit cell (space group $P2_1/n$).

The bite of the oxygen tripod ligand L_{OMe}^-, i.e. the non-bonding distance between the P=O oxygen atoms, is 2.743 to 2.871 Å. This and all the bond distances and angles within the ligand L_{OMe}^- are in the expected range [16–18].

Crystal structure of $[L_{OMe}(CO)Mo(\mu\text{-}CO)Pd(I)C(C_6H_4\text{-}p\text{-}CH_3)C_6H_4\text{-}o\text{-}CH_2N(CH_3)_2]$ (4b)

The molecular structure of the palladium–molybdenum complex **4b**, as determined by a crystal structure study, is shown in Fig. 3. The positional parameters of (**4b**) · $2CH_2Cl_2$ are listed in Table 3, and the main angles and distances for **4b** in Table 4. The molybdenum atom is seven-coordinate, with a distorted 3 : 3 : 1-geometry. The oxygen atoms O7, O8, and O9 of the tripod ligand L_{OMe}^- and the carbon atoms C12, C29, and C30 form a distorted octahedron around molybdenum. The

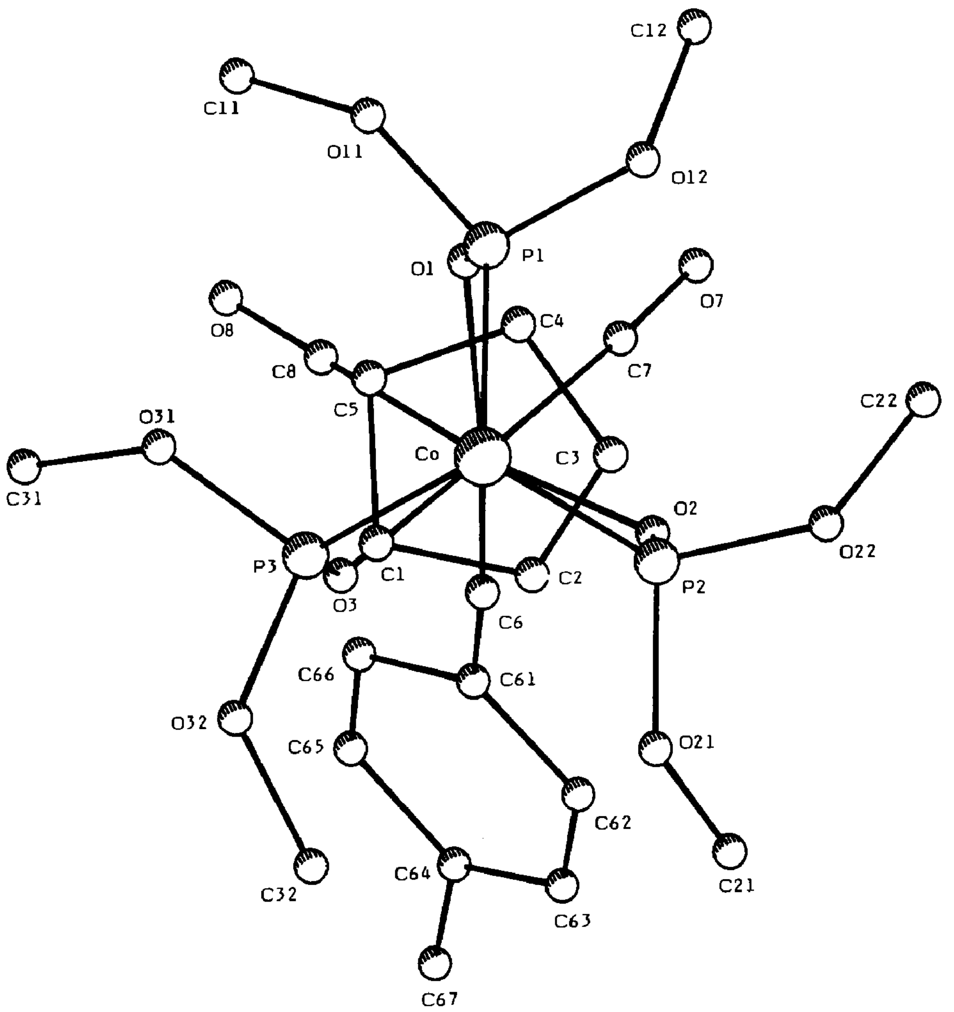

Fig. 2. PLUTO drawing [14] of the molecular structure of $[L_{OMe}(CO)_2W{\equiv}CC_6H_4\text{-}p\text{-}CH_3]$ (**1a**). Projection along the cobalt–tungsten axis. H-atoms are omitted for clarity. The tungsten atom is obscured by the cobalt atom.

palladium atom is situated above the triangular plane formed by the three carbon atoms, and the palladium–molybdenum distance of 2.7619(8) Å is indicative of a strong bonding interaction [19b]. One of the carbonyl ligands with a Pd–C30 distance of 2.265(8) Å can be interpreted as a semi-bridging carbonyl ligand. The second carbonyl ligand with Pd–C29 = 2.672(9) Å is non-bridging. As a consequence of the different bonding modes of the two carbonyl ligands the molybdenum–carbonyl carbon distances (Mo–C29 = 1.966(8), Mo–C30 = 2.009(9) Å) differ slightly. The carbonyl ligands are bent away from the palladium atom, the angles Mo–C29–O10 and Mo–C30–O11 being 169.9(8)° and 163.1(8)°, respectively (see Fig. 3). The oxygen ligand–molybdenum distances (2.129(5), 2.143(6), and 2.210(5) Å) are very similar to the oxygen ligand–tungsten distances in $[L_{OMe}(CO)_2W{\equiv}CC_6H_4\text{-}p\text{-}CH_3]$ (**1a**) (see above). The bite of the oxygen ligand (2.765–2.855 Å) and the P–Co–Mo–O torsional angles are also comparable to the

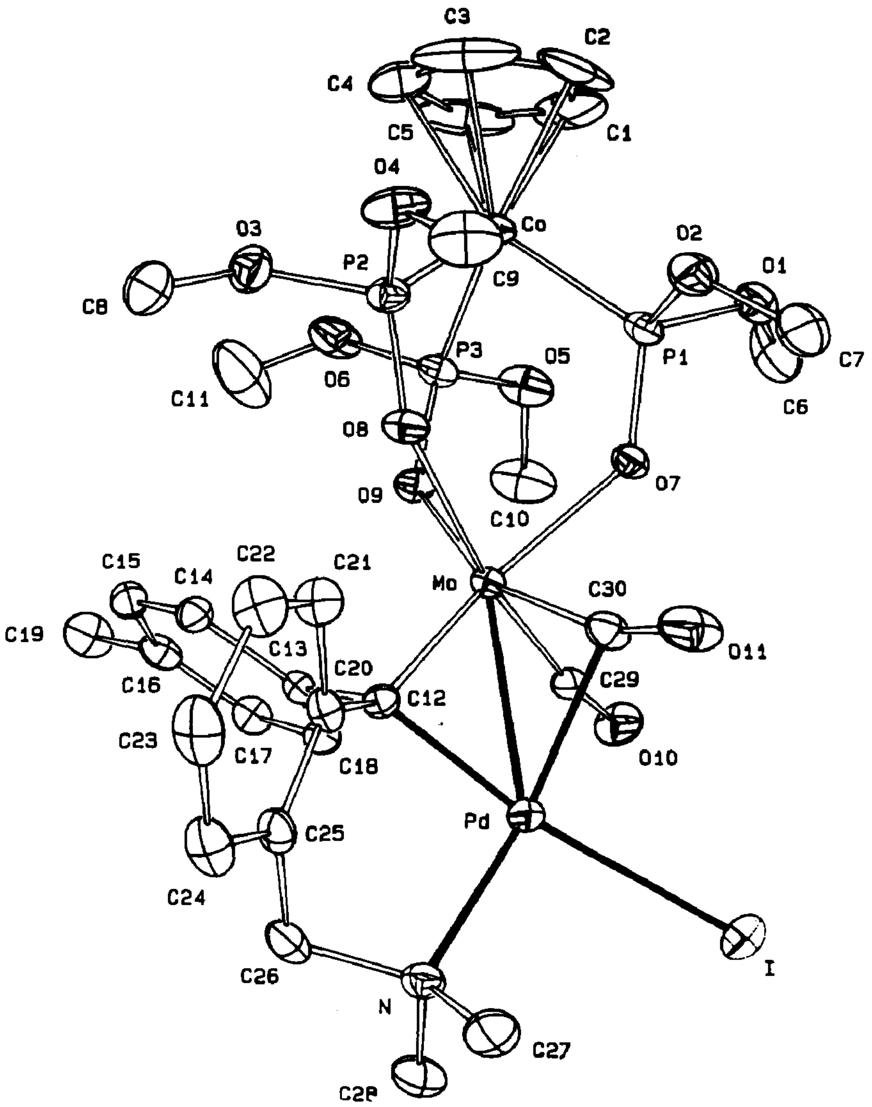

Fig. 3. ORTEP drawing [9] of one molecule of [$L_{OMe}(CO)Mo(\mu\text{-}CO)Pd(I)C(C_6H_4\text{-}p\text{-}CH_3)C_6H_4\text{-}o\text{-}CH_2N(CH_3)_2$] (**4b**) showing the numbering scheme used. Ellipsoids are scaled to enclose 50% of the electronic density. H-atoms and the two co-crystallized CH_2Cl_2-molecules are omitted for clarity.

corresponding values of **1a**. In the unit cell (belonging to the non-centrosymmetric space group $P2_1$) there is only one of the torsional isomers.

Palladium has coordination number five, with C30, I, N, and C12 in a distorted square planar arrangement and molybdenum as the fifth neighbour. The former carbyne carbon atom which has inserted into the palladium–carbon bond of the metallacycle can be described as sp^3 hybridized. The strain induced by the molybdenum–palladium bond at the former carbyne carbon center C12 leads to an acute Mo–C12–Pd angle of 83.9(3)° and an obtuse C20–C12–Mo angle of 138.0(5)°. The Pd–C12 and Mo–C12 distances are in range for single bonds [19,20].

Table 3

Final positional parameters [a] with their estimated standard deviations for [L_{OMe}(CO)Mo(μ-CO)Pd(I)C(C_6H_4-p-CH_3)C_6H_4-o-$CH_2N(CH_3)_2$] (4b)·$2CH_2Cl_2$

Atom	x	y	z	B (Å^2)
I	0.59207(5)	0.780	0.80470(4)	5.05(1)
Pd	0.62346(4)	1.00075(5)	0.85304(3)	3.122(9)
Mo	0.72308(4)	1.15327(5)	0.77576(3)	2.431(9)
Co	0.94741(8)	1.3347(1)	0.69098(6)	3.53(2)
P1	0.9497(1)	1.1580(2)	0.7060(1)	3.56(4)
P2	0.9358(2)	1.3543(2)	0.8174(1)	3.59(4)
P3	0.7587(2)	1.3337(2)	0.6330(1)	3.42(4)
O1	0.9743(5)	1.0905(6)	0.6328(4)	5.5(2)
O2	1.0674(5)	1.1273(6)	0.7835(5)	5.3(2)
O3	0.8933(6)	1.4799(6)	0.8218(4)	5.3(2)
O4	1.0607(5)	1.3598(7)	0.8927(4)	5.9(2)
O5	0.7234(5)	1.2710(8)	0.5431(4)	5.9(2)
O6	0.7085(6)	1.4536(6)	0.6013(4)	6.6(2)
O7	0.8462(4)	1.1042(5)	0.7194(3)	3.4(1)
O8	0.8622(4)	1.2733(5)	0.8442(3)	3.5(1)
O9	0.6883(4)	1.2847(5)	0.6824(3)	3.5(1)
O10	0.5537(5)	0.9982(6)	0.6371(4)	5.3(1)
O11	0.8737(5)	0.9548(7)	0.8838(5)	7.1(2)
C1	1.0219(9)	1.353(1)	0.5989(7)	12.9(3)
C2	1.1078(8)	1.342(1)	0.681(1)	16.5(4)
C3	1.095(1)	1.428(1)	0.7243(8)	12.0(3)
C4	1.013(1)	1.490(1)	0.6779(9)	9.0(3)
C5	0.965(1)	1.443(1)	0.6008(7)	11.6(3)
C6	0.891(1)	1.064(1)	0.5510(8)	8.8(4)
C7	1.0925(8)	1.012(1)	0.8106(8)	6.8(4)
C8	0.889(1)	1.526(1)	0.8969(8)	6.9(3)
C9	1.111(1)	1.273(1)	0.9535(7)	6.9(3)
C10	0.602(1)	1.235(2)	0.4980(7)	8.2(4)
C11	0.641(1)	1.517(2)	0.621(1)	13.5(4)
C12	0.6691(5)	1.1607(6)	0.8833(4)	2.8(1)
C13	0.5903(5)	1.2475(6)	0.8317(4)	2.5(1)
C14	0.6147(6)	1.3630(6)	0.8525(5)	3.3(1)
C15	0.5446(7)	1.4438(7)	0.8028(5)	3.8(2)
C16	0.4471(6)	1.4176(8)	0.7290(5)	3.9(2)
C17	0.4222(6)	1.3100(8)	0.7073(5)	3.9(2)
C18	0.4929(6)	1.2230(7)	0.7595(5)	3.4(1)
C19	0.3718(8)	1.511(1)	0.6785(7)	6.0(2)
C20	0.7228(6)	1.1766(6)	0.9779(4)	3.3(1)
C21	0.8360(7)	1.2169(8)	1.0167(5)	4.1(2)
C22	0.8866(8)	1.232(1)	1.1063(5)	4.9(2)
C23	0.821(1)	1.212(1)	1.1563(6)	5.6(2)
C24	0.7073(8)	1.1697(9)	1.1194(5)	4.8(2)
C25	0.6585(6)	1.1501(7)	1.0291(4)	3.7(1)
C26	0.5386(7)	1.1038(8)	0.9885(5)	4.5(2)
N	0.5364(5)	0.9911(6)	0.9495(4)	3.9(1)
C27	0.6000(9)	0.9091(9)	1.0165(6)	5.5(2)
C28	0.4133(8)	0.957(1)	0.9068(7)	6.0(2)
C29	0.6109(6)	1.0528(6)	0.6933(5)	3.4(1)
C30	0.8037(6)	1.0217(7)	0.8474(5)	3.9(2)
C31	0.306(1)	1.914(2)	0.638(1)	8.8(4)
Cl1	0.2111(4)	1.8082(6)	0.6426(2)	11.7(1)
Cl2	0.2458(4)	2.0438(5)	0.6324(4)	13.0(2)

Table 3 (continued)

Atom	x	y	z	B (Å^2)
C32	0.232(2)	0.331(2)	0.357(1)	9.8(5)
C13	0.3080(5)	0.3100(7)	0.4665(3)	13.8(2)
C14	0.0970(5)	0.2755(6)	0.3267(5)	18.7(2)

[a] Anisotropically refined atoms are given in the form of the isotropic equivalent thermal parameter defined as $(4/3)[a^2B(1,1)+b^2B(2,2)+c^2B(3,3)+ac(\cos\beta)B(1,3)]$.

Table 4

Selected bond angles (deg) and bond distances (Å) with their estimated standard deviations for $[L_{OMe}(CO)Mo(\mu\text{-}CO)Pd(I)C(C_6H_4\text{-}p\text{-}CH_3)C_6H_4\text{-}o\text{-}CH_2N(CH_3)_2]$ (**4b**)

P1–Co–P2	89.86(9)	Co–P1	2.134(3)
P1–Co–P3	90.75(9)	Co–P2	2.165(2)
P2–Co–P3	89.77(8)	Co–P3	2.165(2)
		P1–O7	1.512(5)
		P2–O8	1.500(6)
		P3–O9	1.509(5)
O7–Mo–O8	82.3(2)	Mo–O7	2.129(5)
O7–Mo–O9	82.8(2)	Mo–O8	2.210(5)
O8–Mo–O9	78.8(2)	Mo–O9	2.143(6)
ct–Co–Mo	179.3(1)	ct–Co	1.72(2)
Co–Mo–Pd	165.49(2)		
O7–Mo–C12	150.5(2)		
O8–Mo–C29	167.2(2)		
O9–Mo–C30	158.9(3)		
C12–Mo–C29	104.9(3)	Mo–C12	2.118(7)
C12–Mo–C30	76.9(3)	Mo–C29	1.966(8)
C29–Mo–C30	90.1(4)	Mo–C30	2.009(9)
Mo–C29–O10	169.9(8)	O10–C29	1.15(1)
Mo–C30–O11	163.1(8)	O11–C30	1.17(1)
I–Pd–Mo	122.79(3)	Pd–I	2.7579(8)
I–Pd–C12	170.9(2)	Pd–N	2.227(7)
I–Pd–N	96.1(2)	Pd–C12	2.013(7)
I–Pd–C29	89.1(2)	Pd–Mo	2.7619(8)
I–Pd–C30	97.5(2)	Pd–C29	2.672(9)
Mo–Pd–N	141.0(2)	Pd–C30	2.265(8)
C12–Pd–N	91.9(3)		
C12–Pd–C29	86.3(2)		
C12–Pd–C30	73.5(3)		
N–Pd–C29	148.7(3)		
N–Pd–C30	140.1(3)		
C13–C12–C20	118.4(6)		
Mo–C12–Pd	83.9(3)		
C20–C12–Mo	138.0(5)		
C20–C12–Pd	111.4(5)		

Spectroscopic data

^1H NMR spectra

Very often the symmetry of compounds containing the tris-chelating oxygen ligand L^-_{OMe} can be deduced from analysis of the NMR spectra of L^-_{OMe}. Such a

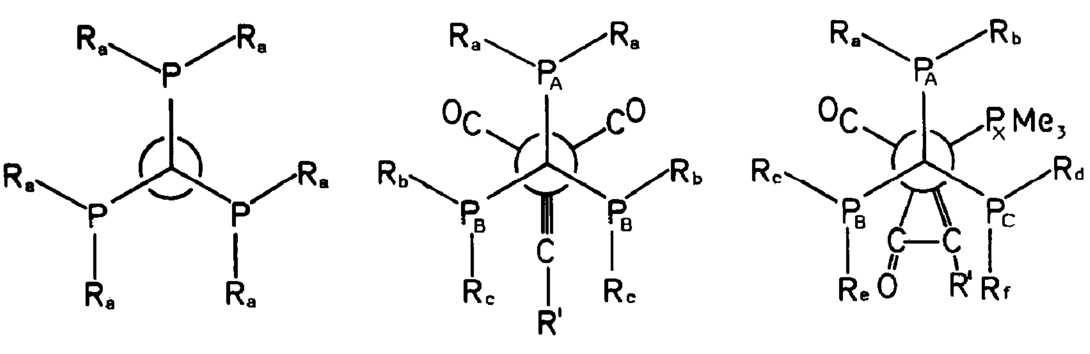

Fig. 4. Parts of the schematic structures of complexes with C_{3v}- (left), C_s- (middle) and C_1-symmetry (right) [21*] (Newman projections along the C_5H_5–Co–M-axis). The alkoxy groups of L_R^- are marked R_a, R_b, R_c, R_d, R_e, and R_f. R′ = C_6H_4-*p*-CH_3.

treatment is presented below for the ^{1}H NMR spectra of the new compounds. The highest possible symmetry that can occur in such complexes is C_{3v}. The six isochronous methoxy groups then give rise to a virtual quartet at $\delta \approx 3.7$ ppm with a coupling ^3J(POCH) ≈ 11 Hz. Coordination of L_R^- to the $[(CO)_2W{\equiv}CC_6H_4\text{-}p\text{-}CH_3]^+$ fragment reduces the symmetry to C_s. For the six groups R we can expect three groups of signals (see Fig. 4, middle). In the complexes **2**, **3a–c**, and **4a**, **b** the

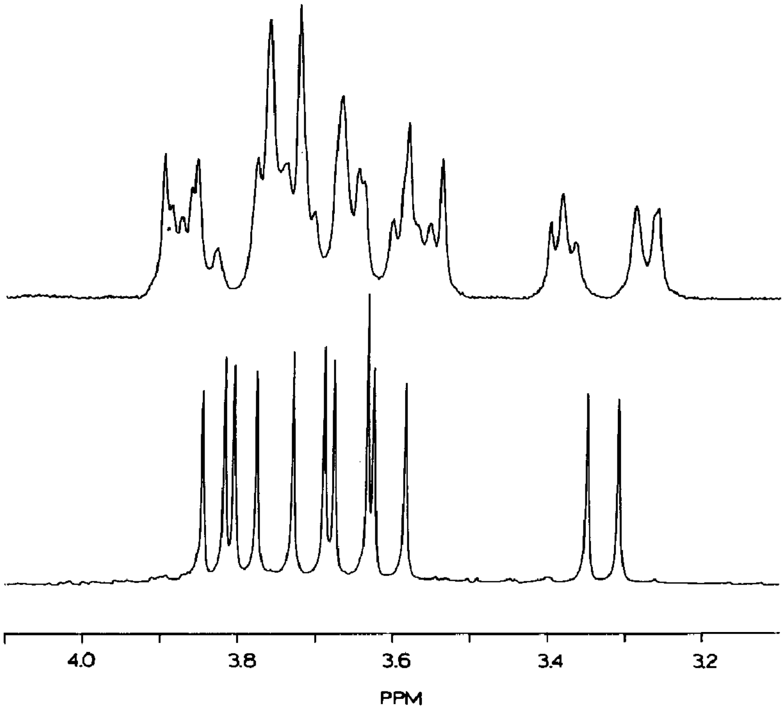

Fig. 5. OCH_3 signals in the 80 MHz (top) and 270 MHz ^{1}H NMR spectrum (bottom) of compound **2**.

---

* Reference number with asterisk indicates a note in the list of references.

symmetry is lowered to C_1, and therefore all six groups R become anisochronous. As an example the ^{1}H NMR spectrum of **2** is shown in Fig. 5. Because of the value of the coupling ^2J(PCoP) constant, 151 Hz, the appearance of the spectrum depends very much on the spectrometer frequency. At 270 MHz the $\Delta\delta$ for the ^{31}P nuclei is large enough to effectively eliminate "virtual" coupling. Therefore six doublets are observed (Fig. 5, bottom spectrum). At 80 MHz, since $\Delta\delta \approx {}^2J$(PCoP) the appearance of the spectrum is markedly changed (Fig. 5, top spectrum).

The complexes **4a, b** are non-rigid. At room temperature the 80 MHz ^{1}H NMR spectra show broad phenyl and featureless methoxy signals that sharpen upon cooling. The 270 MHz spectrum is well resolved, and in accord with the solid state structure (i.e. six non-isochronous methoxy groups, two different *N*-methyl substituents, and an AB system with ^2J(HCH) = 11.2 Hz for the methylene protons). It is noteworthy that even the *p*-tolyl ring shows hindered rotation (ABCD spectrum for the ring protons at low temperature that collapses to a non-resolved $(AM)_2$ spectrum at room temperature. Because of the thermal lability of **4a, b** we could not reach the fast exchange limit, and so we do not yet know the time-averaged symmetry of the molecules and the details of the molecular dynamics. The ^{1}H NMR data for all the new compounds **1–4** are listed in Table 5.

^{31}P and ^{13}C NMR spectra

Depending on the symmetry of the oxygen tripod complexes the ^{31}P{^{1}H} NMR spectra are of the type A_3 (C_{3v}-symmetry, Fig. 4 left), AB_2 (C_s-symmetry, Fig. 4 middle, compounds **1a–e**), or ABC (C_1-symmetry, Fig. 4 right, compounds **2**, **3a–c**, and **4a, b**).

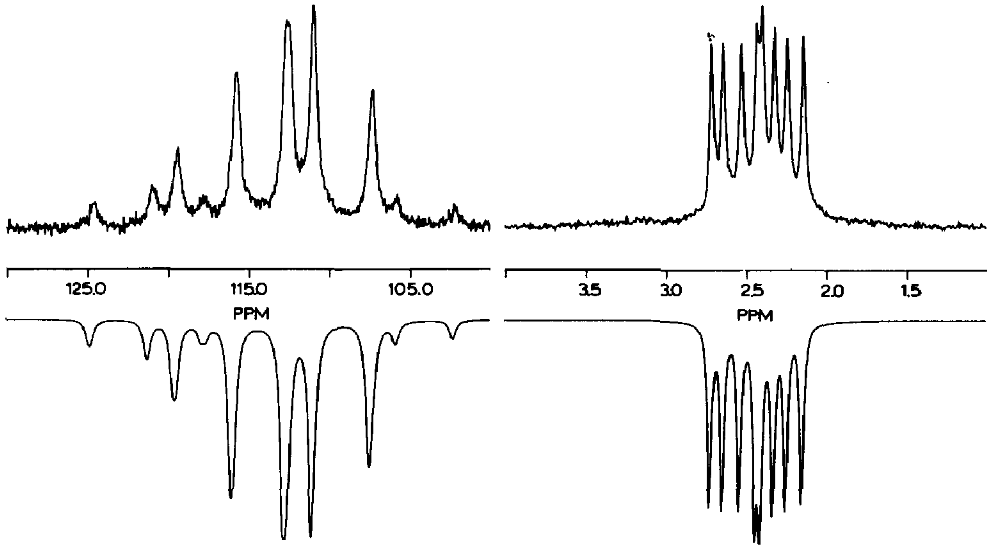

Fig. 6. Measured (above) and calculated (below) 32.4 MHz ^{31}P{^{1}H} NMR spectrum of compound **2**. ABC-part (left) and X-part (right) of the ABCX spin system. The spectrum was calculated by use of the parameters $\delta(P_A)$ = 119.4 ppm, $\delta(P_B)$ = 112.4 ppm, $\delta(P_C)$ = 108.3 ppm, $\delta(P_X)$ = 2.4 ppm, $^2J(P_ACoP_B)$ = $^2J(P_ACoP_C)$ = $^2J(P_BCoP_C)$ = 151 Hz, $^3J(P_AOWP_X)$ = −5.48 Hz, $^3J(P_BOWP_X)$ = −12.06 Hz, $^3J(P_COWP_X)$ = −1.03 Hz.

Table 5

80 MHz ^{1}H NMR data of the complexes **1**–**4** [chemical shifts (ppm), multiplicity, and coupling constants (Hz)]

Compound	$\delta(CH_3)$	$\delta(OCH, OCH_2, OCH_3)$	$\delta(C_5H_5)$	$\delta(p\text{-}CH_3)$
1b	1.28(t ^{a}, 7.0 Hz)	3.84–4.39(m)	5.00(q ^{b}, 0.4 Hz)	2.22(s)
1d	1.28(t ^{a}, 7.1 Hz)	3.89–4.39(m)	4.98(q ^{b}, 0.4 Hz)	2.26(s)
1e	1.13–1.50(m)	4.60–5.11(m)	4.84(q ^{b}, 0.4 Hz)	2.25(s)
2	–	3.23–3.93(m)	5.08(q ^{b}, 0.4 Hz)	2.33(s)
2 ^{e}	–	3.33(d ^{f}, 11.0 Hz, 3H)	5.09(s)	2.33(s)
		3.60(d ^{f}, 11.0 Hz, 3H)		
		3.65(d ^{f}, 11.6 Hz, 3H)		
		3.71(d ^{f}, 10.9 Hz, 3H)		
		3.80(d ^{f}, 11.2 Hz, 3H)		
		3.83(d ^{f}, 11.0 Hz, 3H)		
3a	–	3.43–3.90(m)	5.00(s)	2.19(s)
3b	1.26(t ^{a}, 7.1 Hz)	3.78–4.39(m)	4.97(s)	2.20(s)
3c	1.27–1.37(m)	4.76–4.91(m)	4.81(q ^{b}, 0.4 Hz)	2.20(s)
4a ^{e}	–	3.19(d ^{f}, 9.2 Hz, 3H)	5.02(s)	2.26(s)
		3.54(d ^{f}, 11.7 Hz, 3H)		
		3.69(d ^{f}, 9.1 Hz, 6H)		
		3.82(d ^{f}, 10.2 Hz, 6H)		
4b ^{e}	–	3.17(d ^{f}, 11.3 Hz, 3H)	4.99(s)	2.27(s)
		3.47(d ^{f}, 11.5 Hz, 3H)		
		3.62(d ^{f}, 11.3 Hz, 3H)		
		3.76(d ^{f}, 11.0 Hz, 3H)		
		3.77(d ^{f}, 11.2 Hz, 3H)		
		3.81(d ^{f}, 11.3 Hz, 3H)		

[a] $^{3}J(HCCH)$. [b] $^{3}J(PCoCH)$. [c] $(AB)_2$ spectrum. $^{3}J(H_ACCH_B) \approx 8.1$ Hz. [d] $^{2}J(PCH)$. [e] 270 MHz ^{1}H NMR. [f] $^{3}J(POCH)$. [g] $^{2}J(HCH)$. [h] $^{4}J(HCCCH)$.

The phosphorus nucleus of the additional trimethylphosphine ligand in the compounds **2** and **3a**–**c** is coupled to the three phosphorus nuclei of the tripod ligand. The experimental and the calculated ABCX spectra of **2** are shown in Fig. 6. The largest coupling constant for the phosphine phosphorus is, as expected, the one for the phosphite in a *trans* position.

The data from the proton-decoupled ^{13}C NMR spectra (chemical shifts and ^{13}C–^{31}P coupling constants) are given in Table 6. The changes in chemical shifts observed upon introduction of a trimethylphosphine ligand are similar to those for the cyclopentadienyl complexes reported by Kreissl et al. [7]. The electron-donating effect of the ligands L_R^- in these compounds, however, seems to be stronger than that for any other reported monoanionic 6e$^-$-ligand. As a consequence of the increased back bonding the metal carbonyl carbon signals appear at higher chemical shifts than those from the related cyclopentadienyl [22], pentamethylcyclopentadienyl [23], and poly(pyrazolyl)borate compounds [13]. The tungsten carbonyl and the ketenyl carbonyl signals of compound **2** appear as singlets at $\delta = 230.9$ and 208.1 ppm, respectively. The ketenyl carbon at $\delta = 204.7$ ppm is coupled to the phosphine with $^{2}J(PWC) = 9.5$ Hz.

δ(p-C_6H_4)	δ(PMe_3)	δ(NCH_3)	δ(NCH_2)	δ(o-C_6H_4)
6.96, 7.08 [c]				
6.97, 7.19 [c]				
6.96, 7.16 [c]				
7.17, 7.89 [c]	1.27(d [d], 9.4 Hz)			
7.17, 7.89 [c]	1.27(d [d], 9.4 Hz)			
6.84, 7.08 [c]	1.34(d [d], 8.3 Hz)			
6.86, 7.06 [c]	1.32(d [d], 8.5 Hz)			
6.84, 7.05 [c]	1.31(d [d], 8.8 Hz)			
6.83(d [a], 6.9 Hz)		2.37(s)	2.98, 3.06 (AB [g], 11.2 Hz)	7.23–7.24(m, 2H)
6.90(d [a], 8.5 Hz)		2.64(s)		7.39–7.46(m, 1H)
7.33(d [a], 8.7 Hz)				8.28(d [a], 7.7 Hz, 1H)
8.09(d [a], 7.7 Hz)				
6.91(d [b], 6.4 Hz)		2.45(s)	2.92, 3.05 (AB [g], 11.2 Hz)	7.23(d [a]/d [h], 6.7/1.5 Hz)
6.94(d [a], 8.3 Hz)		2.70(s)		7.30(d [a]/d [h], 7.3/1.3 Hz)
7.32(d [a], 9.6 Hz)				7.46(d [a]/t [h], 7.4/1.6 Hz)
7.92(d [a], 7.2 Hz)				8.46(d [a]/d [h], 7.5/1.0 Hz)

IR spectra

The IR spectra of compounds **1**–**4** show the characteristic absorption pattern for the tripod ligands L_R^-. The additional bands of the carbonyl ligands are listed in Table 7. The carbyne complexes **1a**–**e** have two ν(CO) bands at rather low frequencies ($\approx$ 1860/1960 cm^{-1}). In the series $C_5H_5^- > C_5Me_5^- \approx B(pz)_4^- \approx HB(pz)_3^- \gg L_R^-$ the ν(CO) frequencies are lower by about 25 to 50 cm^{-1} in this type of compound. Coordination of a trimethylphosphine ligand lowers the ν(CO) frequency to ca. 1947 cm^{-1} for **3a**–**c** and 1840 cm^{-1} for the η^2 ketenyl complex **2**. The ketenyl carbonyl gives a band at 1685 cm^{-1}. The addition of a (dmba)PdI unit to the carbyne complexes **1a**, **c** to give the complexes **4** changes the electronic properties significantly. This is evident from the change in the ν(CO) frequencies. In the IR spectra of the products **4** they appear as two broad bands at 1912 and 1823 cm^{-1} (**4a**, M = W) or 1930 and 1836 cm^{-1} (**4b**, M = Mo), whereas in the spectra of the starting compounds **1** they are observed at 1961 and 1859 cm^{-1} (**1a**, M = W) or 1977 and 1881 cm^{-1} (**1c**, M = Mo).

Table 6

$^{13}C\{^{1}H\}$ NMR data of the complexes **1–3** [chemical shifts (ppm), multiplicity, and coupling constants (Hz)]

Compound	δ(M≡C)	δ(CO)	$\delta(C_6H_4)$	$\delta(C_5H_5)$	$\delta(OCH, OCH_2, OCH_3)$	$\delta(CH_3)$	δ(*p*-CH_3)	$\delta(PMe_3)$	δ(ketenyl–CO)	δ(ketenyl–C)
1b	278.1	229.7	148.3, 136.0, 128.7, 128.1	89.4	62.2–60.5(m)	16.6	21.5			
1d	287.1	230.2	144.3, 137.3, 128.5, 128.3	89.2	61.4–60.0(m)	16.7	21.6			
1e	286.1	230.7	144.3, 136.9, 129.3, 128.4	89.6	68.4	24.6	21.5			
2	–	230.9	137.9, 135.3, 128.9, 127.4	89.0	53.7(d ^{a}, 8.7 Hz) 53.4(d ^{a}, 9.8 Hz) 53.0(d ^{a}, 10.1 Hz) 52.7(d ^{a}, 9.5 Hz) 52.1(d ^{a}, 7.5 Hz) 51.6(d ^{a}, 9.1 Hz)	–	21.4	17.0 (d ^{b}, 30.6 Hz)	208.1	204.7 (d ^{c}, 9.5 Hz)
3a	279.4 (d ^{c}, 26.5 Hz)	256.5 (d ^{c}, 13.3 Hz)	145.2, 133.6, 127.8, 126.7	88.4	53.0–51.0(m)		21.2	18.2 (d ^{b}, 24.1 Hz)		
3b	278.8 (d ^{c}, 25.7 Hz)	257.0 (d ^{c}, 14.7 Hz)	145.5, 133.5, 127.9, 126.8	88.9	62.6–59.3(m)	16.7	21.3	18.4 (d ^{b}, 23.7 Hz)		

[a] ^{2}J(POC). [b] ^{1}J(PC). [c] ^{2}J(PWC).

Table 7

ν(CO)-frequencies (cm^{-1}) of the complexes **1–4**

Compound	ν(CO) ^{a}	ν(CO) ^{b}
$[L_{OEt}(CO)_2W{\equiv}CC_6H_4\text{-}p\text{-}CH_3]$ (**1b**)	1958, 1858	1958, 1856
$[L_{OEt}(CO)_2Mo{\equiv}CC_6H_4\text{-}p\text{-}CH_3]$ (**1d**)	1973, 1878	1984, 1894 ^{c}
$[L_{O\text{-}i\text{-}Pr}(CO)_2Mo{\equiv}CC_6H_4\text{-}p\text{-}CH_3]$ (**1e**)	1969, 1877	1982, 1893 ^{c}
$[L_{OMe}(CO)\{P(CH_3)_3\}W(\eta^2\text{-}C(O)CC_6H_4\text{-}p\text{-}CH_3)]$ (**2**)	1840, 1685	1851, 1681
$[L_{OMe}(CO)\{P(CH_3)_3\}Mo{\equiv}CC_6H_4\text{-}p\text{-}CH_3]$ (**3a**)	1850, 1839	1856 ^{d}
$[L_{OEt}(CO)\{P(CH_3)_3\}Mo{\equiv}CC_6H_4\text{-}p\text{-}CH_3]$ (**3b**)	1849	
$[L_{O\text{-}i\text{-}Pr}(CO\{P(CH_3)_3\}Mo{\equiv}CC_6H_4\text{-}p\text{-}CH_3]$ (**3c**)	1847	1868 ^{c}
$[L_{OMe}(CO)W(\mu\text{-}CO)Pd(I)C(C_6H_4\text{-}p\text{-}CH_3)C_6H_4\text{-}o\text{-}CH_2N(CH_3)_2]$ (**4a**)	1905, 1811	1912, 1823
$[L_{OMe}(CO)Mo(\mu\text{-}CO)Pd(I)C(C_6H_4\text{-}p\text{-}CH_3)C_6H_4\text{-}o\text{-}CH_2N(CH_3)_2]$ (**4b**)	1922, 1835	1930, 1836

[a] KBr. [b] Dichloromethane. [c] Hexane. [d] Diethyl ether.

Experimental section

Reagents and general techniques

All reactions were performed under dry nitrogen in conventional Schlenk glassware. Infrared spectra were recorded on a Perkin-Elmer PE 580 spectrometer. The rotational lines of dilute gaseous deuterium chloride and deuterium bromide were used to calibrate the CO stretching frequencies [24]. NMR spectra were obtained on a Bruker WP80 SY (^1H, ^{31}P) and Bruker WH270 (^1H, ^{13}C) NMR spectrometer. The spectroscopic data for the new compounds are shown in Tables 5, 6 and 7. The compounds $[N(CH_3)_4][(CO)_5M{=}C(O)(C_6H_4\text{-}p\text{-}CH_3)]$ [25], *trans*-$Br(CO)_4M{\equiv}CC_6H_4\text{-}p\text{-}CH_3$ (M = Mo, W) [26], $P(CH_3)_3$ [27], $[\{(dmba)PdI\}_2]$ [6a], $[L_{OMe}(CO)_2M{\equiv}CC_6H_4\text{-}p\text{-}CH_3]$ (M = Mo, W) [5], and the sodium salts of the oxygen tripod ligands NaL_{OEt} [16] and $NaL_{O\text{-}i\text{-}Pr}$ [28] were prepared by published methods.

Syntheses

$[(C_5H_5)Co\{P(O)(OC_2H_5)_2\}_3(CO)_2W{\equiv}CC_6H_4\text{-}p\text{-}CH_3]$ (1b). A solution of *trans*-$Br(CO)_4W{\equiv}CC_6H_4\text{-}p\text{-}CH_3$ in dichloromethane was prepared from 0.79 g (1.52 mmol) of $[N(CH_3)_4][(CO)_5W{=}C(O)(C_6H_4\text{-}p\text{-}CH_3)]$ and 0.15 ml (1.60 mmol) of oxalyl bromide [26] and 0.85 g (1.52 mmol) of NaL_{OEt} was added. Gas was evolved, and the solution turned dark red within a few hours. The completion of the reaction was checked by IR spectroscopy. The solvent was removed in vacuo and the solid residue chromatographed on a column of silica (15 × 2 cm). The product eluted with dichloromethane as an orange-red band was dried in vacuo. A diethyl ether solution of the product was cooled to −35 °C. After two days the orange-red crystals formed were filtered off, washed with little hexane, and dried in vacuo: yield 0.61 g (46%).

$[(C_5H_5)Co\{P(O)(OC_2H_5)_2\}_3(CO)_2Mo{\equiv}CC_6H_4\text{-}p\text{-}CH_3]$ (1d). This was prepared in the same manner as **1b** from 1.56 g (3.63 mmol) of $[N(CH_3)_4][(CO)_5Mo{=}C(O)C_6H_4\text{-}p\text{-}CH_3)]$, 0.35 ml (3.70 mmol) of oxalyl bromide, and 2.03 g (3.63 mmol) of NaL_{OEt}. Recrystallization from hexane at −35 °C gave 1.86 g (65%) of orange-red crystals. Anal. Found: C, 41.05; H, 5.36. $C_{27}H_{42}CoMoO_{11}P_3$ (790.42) calcd.: C, 41.03; H, 5.36%.

$[(C_5H_5)Co\{P(O)(O\text{-}i\text{-}C_3H_7)_2\}_3(CO)_2Mo{\equiv}CC_6H_4\text{-}p\text{-}CH_3]$ (1e). This was prepared in the same manner as **1b** from 1.10 g (2.55 mmol) of $[N(CH_3)_4][(CO)_5Mo{=}C(O)(C_6H_4\text{-}p\text{-}CH_3]$, 0.24 ml (2.60 mmol) of oxalyl bromide, and 1.64 g (2.55 mmol) of $NaL_{O\text{-}i\text{-}Pr}$. The yield after recrystallization from hexane at −35 °C was 1.10 g (49.5%) of orange-red crystals. Anal. Found: C, 45.31; H, 6.25. $C_{33}H_{54}CoMoO_{11}P_3$ (874.58) calcd.: C, 45.32; H, 6.22%.

$[(C_5H_5)Co\{P(O)(OCH_3)_2\}_3(CO)\{P(CH_3)_3\}W(\eta^2\text{-}C(O)CC_6H_4\text{-}p\text{-}CH_3)] \cdot CH_2Cl_2$ ($2 \cdot CH_2Cl_2$). To a stirred solution of 0.41 g (0.51 mmol) of $[L_{OMe}(CO)_2W{\equiv}CC_6H_4\text{-}p\text{-}CH_3]$ in 15 ml of dichloromethane was added 0.16 ml (1.69 mmol) of trimethylphosphine. As judged from the IR spectra the reaction was nearly complete after ca. 150 h. The mixture was then evaporated to dryness under reduced pressure. The oily brown residue was taken up in dichloromethane and chromatographed on a silica column. Acetone (ca. 100 ml) eluted the product as a broad violet band. Recrystallization from dichloromethane/hexane (1/3) yielded large violet crystals, which were washed with hexane and dried in vacuo [0.31 g (64%)]. The compound is soluble in dichloromethane, acetone, and THF, and insoluble in diethyl ether and hexane. Anal. Found: C, 31.55; H, 4.37. $C_{24}H_{39}Cl_2CoO_{11}P_4W$ (955.18) calcd.: C, 31.44; H, 4.33%. $^{31}P\{^1H\}$ NMR (32.4 MHz, $CDCl_3$, −58 °C): δ (ppm) 119.2 (P_A, $^2J(P_ACoP_B)$

$= {}^2J(P_ACoP_C) = 151$ Hz, ${}^3J(P_AOWP_X) = -5.48$ Hz); 112.3 (P_B, ${}^2J(P_BCoP_C) = 151$ Hz, ${}^3J(P_BOWP_X) = -12.06$ Hz); 108.2 (P_C, ${}^3J(P_COWP_X) = -1.03$ Hz); 2.4 (d · d · d with ^{183}W-satellites, ${}^1J({}^{183}W-{}^{31}P)$ 404 Hz, P_X).

*$[(C_5H_5)Co\{P(O)(OCH_3)_2\}_3(CO)\{P(CH_3)_3\}Mo{\equiv}CC_6H_4\text{-}p\text{-}CH_3)$ (**3a**).* To a stirred solution of 0.06 g (0.09 mmol) of $[L_{OMe}(CO)_2Mo{\equiv}CC_6H_4\text{-}p\text{-}CH_3]$ in 2.5 ml of toluene was added 0.01 g (1.45 mmol) of trimethylphosphine. The mixture turned dark violet within about 1 h, but, as judged by the IR spectrum, the reaction was complete only after 3 days. After removal of the solvent the residue was crystallized from diethyl ether at −35 °C to give a microcrystalline violet solid. The compound is freely soluble in dichloromethane and diethyl ether and slightly soluble in hexane. ${}^{31}P({}^1H)$ NMR (32.4 MHz, $CDCl_3$, −58 °C): δ (ppm) 111.5 (m, ABC-part of an ABCX-spin system); 23.4 (q, X-part of an ABCX-spin system, $P(CH_3)_3$).

*$[(C_5H_5)Co\{P(O)(OC_2H_5)_2\}_3(CO)\{P(CH_3)_3\}Mo{\equiv}CC_6H_4\text{-}p\text{-}CH_3]$ (**3b**).* Trimethylphosphine (0.11 ml, 1.16 mmol) was added to a stirred solution of 0.23 g (0.36 mmol) of $[L_{OEt}(CO)_2Mo{\equiv}C\text{-}C_6H_4\text{-}p\text{-}CH_3\}$ in 10 ml of hexane. The mixture, which slowly turned dark, was stirred until the reaction was complete (IR monitoring). The solvent was then distilled off in vacuo and the oily violet residue was taken up in a little hexane. Cooling overnight to −78 °C yielded a violet precipitate, which was filtered off and dried in vacuo. [0.26 g (84%)]. The compound is soluble in most organic solvents. ${}^{31}P\{{}^1H\}$ NMR (32.4 MHz, $CDCl_3$, −58 °C): δ (ppm) 104.4–112.8 (m, ABC-part of an ABCX-spin system); 21.3–25.9 (q, X-part of an ABCX-spin system, $P(CH_3)_3$).

*$[(C_5H_5)Co\{P(O)(O\text{-}i\text{-}C_3H_7)_2]_3(CO)\{P(CH_3)_3\}Mo{\equiv}CC_6H_4\text{-}p\text{-}CH_3]$ (**3c**).* To a stirred solution of 0.44 g (0.50 mmol) of $[L_{O\text{-}i\text{-}Pr}(CO)_2Mo{\equiv}CC_6H_4\text{-}p\text{-}CH_3]$ in hexane was added 0.2 ml (2.1 mmol) of trimethylphosphine. After 200 h a small amount of silica was added and the volatile species were distilled off in vacuo. The residual violet powder was chromatographed on a silica column (15 × 2.5 cm) and the product eluted with ether as a broad violet band. Evaporation of the solvent left **3c** as violet powder. The compound is very soluble in most organic solvents.

*$[L_{OMe}(CO)\overline{W(\mu\text{-}CO)}\overline{\underline{Pd(I)C}}\underline{(C_6H_4\text{-}p\text{-}CH_3)C_6H_4\text{-}o\text{-}CH_2N}(CH_3)_2] \cdot 2CH_2Cl_2$ (**4a** · $2CH_2Cl_2$).* A solution of 0.16 g (0.2 mmol) of $[L_{OMe}(CO)_2W{\equiv}CC_6H_4\text{-}p\text{-}CH_3]$ and 0.08 g (0.1 mmol) of $[\{(dmba)PdI\}_2]$ in 15 ml of dichloromethane was kept in the dark for 24 h, then concentrated and filtered through a membrane to remove small particles. The filtrate was covered with a layer of hexane and set aside in the dark for several days. The solvent was then decanted from the large dark brown to black needle-like crystals, which were washed with a little ether and dried in vacuo. Yield: 0.20 g (75%). The compound is soluble in dichloromethane, acetone, and chloroform, but insoluble in diethyl ether and hexane. Anal. Found: C, 28.58; H, 3.39; N, 1.04. $C_{32}H_{46}Cl_4CoINO_{11}P_3PdW$ (1331.54) calcd.: C, 28.08; H, 3.41; N, 1.04%. ${}^{31}P\{{}^1H\}$ NMR (32.4 MHz, CH_2Cl_2, −69 °C): δ (ppm) 119.40 (P_A, ${}^2J(P_ACoP_B) = {}^2J(P_ACoP_C) = 151$ Hz); 117.6 (P_B, ${}^2J(P_BCoP_C) = 151$ Hz); 107.98 (P_C).

*$[L_{OMe}(CO)\overline{Mo(\mu\text{-}CO)}\overline{\underline{Pd(I)C}}\underline{(C_6H_4\text{-}p\text{-}CH_3)C_6H_4\text{-}o\text{-}CH_2N}(CH_3)_2] \cdot 2CH_2Cl_2$ (**4b** · $2CH_2Cl_2$).* This compound was made in the same way as **4a** from 0.24 g (0.33 mmol) of $[L_{OMe}(CO)_2Mo{\equiv}C\text{-}C_6H_4\text{-}p\text{-}CH_3]$ and 0.12 g (0.17 mmol) of $[\{(dmba)PdI\}_2]$ in 10 ml of dichloromethane. The yield was 0.12 g (29%) of shiny dark brown needles. The compound is soluble in dichloromethane, acetone, chloroform, and insoluble in diethyl ether and hexane. Anal. Found: C, 31.07; H, 3.76; N, 1.11. $C_{32}H_{46}Cl_4CoIMoNO_{11}P_3Pd$ (1243.63) calcd.: C, 30.91; H, 3.73; N, 1.13%. ${}^{31}P\{{}^1H\}$ NMR (32.4 MHz, CD_3COCD_3, −69 °C): δ (ppm) 126.55 (P_A, ${}^2J(P_ACoP_B) = {}^2J(P_ACoP_C) = 151$ Hz); 120.70 (P_B, ${}^2J(P_BCoP_C) = 151$ Hz); 113.55 (P_C).

$^{31}P\{^1H\}$ NMR (32.4 MHz, CD_3COCD_3, −69 °C): δ (ppm) 126.55 (P_A, $^2J(P_ACoP_B) = {}^2J(P_ACoP_C) = 151$ Hz); 120.70 (P_B, $^2J(P_BCoP_C) = 151$ Hz); 113.55 (P_C).

X-ray data collection and structure determinations

[$L_{OMe}(CO)_2W{\equiv}CC_6H_4$-p-$CH_3$]. A suitable crystal of [$L_{OMe}(CO)_2W{\equiv}CC_6H_4$-*p*-$CH_3$] (**1a**) was obtained from dichloromethane/diethyl ether and sealed in a capillary tube. Weissenberg and precession photographs showed that crystals of **1a** belong to the monoclinic system, space group $P2_1/n$. Unit cell dimensions (Table 8) were determined by least-squares refinement of the best angular positions for 25 independent reflexions (10° < θ < 19°) using monochromatized Mo-K_α radiation. Data were collected on an Enraf-Nonius CAD4-diffractometer; the parameters are given in Table 8. The intensities of three standard reflexions were remeasured after every three hours. The intensities of these reflexions showed a total loss of 16% and were corrected to the closest standards. Data were corrected for Lorentz and polarization effects. An empirical absorption correction was applied using the Psi-scan method [29] and symmetry-related reflexions were averaged. The structure was solved by the heavy atom method and difference-Fourier synthesis using the program SDP [30] on a VAX 11/730 computer (Digital Equipment Corp.). All non-hydrogen atoms were refined anisotropically. The hydrogen atoms were placed

Table 8

X-ray experimental parameters

	Compound **1a**	Compound **4b**
Formula	$C_{21}H_{30}CoO_{11}P_3W$	$C_{32}H_{46}Cl_4CoIMoNO_{11}P_3Pd$
Molecular weight, g/mol	794.2	1243.6
Color	orange	dark brown
Crystal size, mm	1.00×0.32×0.15	0.33×0.28×0.21
Cryst. system	monoclinic	monoclinic
Space group, No.	$P2_1/n$, No. 14	$P2_1$, No. 4
a, Å	10.529(1)	12.286(2)
b, Å	21.148(6)	12.004(4)
c, Å	13.038(3)	16.590(3)
β, deg	95.63(1)	111.18(2)
V, $Å^3$	2889(2)	2281.5
Z (molecules/cell)	4	2
d_{calc}, g/cm^3	1.826	1.807
Radiation	Mo-K_α	Mo-K_α
Monochromator	graphite	graphite
μ, cm^{-1}	48.52	20.68
Temperature, °C	20	20
Scan mode	$\omega - 2\theta$	$\theta/2\theta$
Scan range θ, deg	$1.2 + 0.35 \tan(\theta)$	$0.90 + 0.34 \tan(\theta)$
2θ range, deg	< 30	2.5/30
Octants	$+h+k\pm l$	$\pm h+k+l$
No. of data collected	8842	7124
No. of data with $I > 3\sigma(I)$	5199	4515
No. of parameters	335	495
$R(F)$	0.058	0.032
$R_w(F)$	0.073	0.048
Instrumental error factor p	0.04	0.07
GOF	2.683	1.126

in calculated positions ($d_{C-H} = 0.95$ Å) and treated as riding atoms with fixed thermal parameters ($B_{iso} = 10$ Å^2). The structure was refined by full-matrix least-squares techniques leading to the final values of $R = 5.8\%$ and $R_w = 7.3\%$ (statistical weights used).

$[L_{OMe}(CO)Mo(\mu\text{-}CO)Pd(I)C(C_6H_4\text{-}p\text{-}CH_3)C_6H_4\text{-}o\text{-}CH_2N(CH_3)_2]$. Suitable single crystals of **4b** were obtained from dichloromethane/hexane. A single crystal was cut out from a cluster of material and mounted on a standard goniometer head. A systematic search in reciprocal space using a Enraf-Nonius CAD4-F automatic diffractometer showed that crystals of **4b** belong to the monoclinic system. Quantitative data were obtained at room temperature. All experimental parameters used are given in Table 8. The resulting data-set was transferred to a VAX computer, and for all subsequent calculations the Enraf-Nonius SDP/VAX package [30] was used. Three standard reflexions measured every hour during the entire data collection period showed no significant trend. The data were converted to intensities and then corrected for Lorentz and polarization factors. The structure was solved using the heavy atom method. After refinement of the non-hydrogen atoms, a difference-Fourier map revealed maximas of residuals electronic density close to the positions expected for hydrogen atoms; they were introduced in structure factor calculations by their computed coordinates ($d_{C-H} = 0.95$ Å) and isotropic temperature factors such as $B(H) = 1.3B_{iso}(C)$ Å^2 but not refined. At this stage empirical absorption corrections were applied by use of Walker and Stuart's method [31] since face indexation was not possible. The absolute structure was determined by comparing the refinements of the x, y, z and $-x$, $-y$, $-z$ coordinates sets. Full least-squares refinements; $\sigma^2(F^2) = \sigma^2(\text{counts}) + (pI)^2$. A final difference map revealed no significant maxima. The scattering factor coefficients and anomalous dispersion coefficients were taken from refs. 32a and 32b, respectively.

Supplementary material

Tables of hydrogen atom coordinates, thermal parameters, complete lists of bond lengths and angles, and lists of observed and calculated structure factors are available from FIZ, Fachinformationszentrum Energie, Physik, Mathematik GmbH, D-7514 Eggenstein-Leopoldshafen 2, upon full citation of this article (registration number CSD 54650).

Acknowledgement

Our work is supported by the Fonds der chemischen Industrie (to W.K.) and by the CNRS (to M.P.). We thank Bayer AG Leverkusen for a gift of valuable chemicals, Dr. N. Klaff for his help with the crystal structure determination of $[L_{OMe}(CO)_2W{\equiv}CC_6H_4\text{-}p\text{-}CH_3]$, and A. Hesse and H.-J. Schulte for their skilled preparations of some of the compounds.

References and notes

1 E.O. Fischer, G. Kreis, C.G. Kreiter, J. Müller, G. Huttner and H. Lorenz, Angew. Chem., 85 (1973) 618; Angew. Chem., Int. Ed. Engl., 12 (1973) 564.
2 H. Fischer, P. Hoffmann, F.R. Kreissl, R.R. Schrock, U. Schubert and K. Weiss (Eds.), Carbyne Complexes, Verlag Chemie, Weinheim, 1988.
3 F.G.A. Stone, Angew. Chem., 96 (1984) 85; Angew. Chem., Int. Ed. Engl., 23 (1984) 89.
4 S.J. Davies, J.A.K. Howard, M.U. Pilotti and F.G.A. Stone, J. Chem. Soc., Dalton Trans., (1989) 2289 and refs. therein.

5 W. Kläui and H. Hamers, J. Organomet. Chem., 345 (1988) 287.

6 (a) F. Maassarani, M. Pfeffer and G. Le Borgne, Organometallics, 6 (1987) 2029; (b) J. Dupont, M. Pfeffer, J.-C. Daran and J. Gouteron, J. Chem. Soc., Dalton Trans., (1988) 2421; (c) J. Dupont, M. Pfeffer, M.A. Rotteveel, A. de Cian and J. Fischer, Organometallics, 8 (1989) 1116; (d) M. Pfeffer, M.A. Rotteveel, J.-P. Sutter, A. de Cian and J. Fischer, J. Organomet. Chem., 371 (1989) C21; (e) M.T. Pereira, M. Pfeffer and M.A. Rotteveel, J. Organomet. Chem., 375 (1989) 139; (f) M. Pfeffer and M.A. Rotteveel, Recl. Trav. Chim. Pays-Bas, 108 (1989) 317; (g) N. Beydoun and M. Pfeffer, Synthesis, in press.

7 (a) F.R. Kreissl, P. Friedrich and G. Huttner, Angew. Chem., 89 (1977) 110; Angew. Chem., Int. Ed. Engl., 16 (1977) 102. (b) F.R. Kreissl, K. Eberl and W. Uedelhoven, Chem. Ber., 110 (1977) 3782; (c) W. Uedelhoven, K. Eberl and F.R. Kreissl, Chem. Ber., 112 (1979) 3376; (d) F.R. Kreissl, W. Uedelhoven and D. Neugebauer, J. Organomet. Chem., 344 (1988) C27.

8 P.M. Maitlis, J. Organomet. Chem., 200 (1980) 161.

9 C.K. Johnson, ORTEP: A Fortran thermal-ellipsoid plot program for crystal structure illustrations, third revision, Oak Ridge National Laboratory, ORNL-5138, Oak Ridge, TN, 1976.

10 E.O. Fischer, T.L. Lindner, G. Huttner, P. Friedrich, F.R. Kreissl and J.O. Besenhard, Chem. Ber., 110 (1977) 3397.

11 M. Green, J.A.K. Howard, A.P. James, A.N. de M. Jelfs, C.M. Nunn and F.G.A. Stone, J. Chem. Soc., Chem. Commun., (1984) 1623.

12 F.-R. Baumann, J.A.K. Howard, O. Johnson and F.G.A. Stone, J. Chem. Soc., Dalton Trans., (1987) 2661.

13 M. Green, J.A.K. Howard, A.P. James, C.M. Nunn and F.G.A. Stone, J. Chem. Soc., Dalton Trans., (1986) 187.

14 W.D.S. Motherwell and W. Clegg, PLUTO: A program for plotting molecular and crystal structures, Univ. of Cambridge, England, 1978.

15 O. Ermer and J.D. Dunitz, Helv. Chim. Acta, 52 (1969) 1861.

16 W. Kläui, B. Lenders, B. Hessner and K. Evertz, Organometallics, 7 (1988) 1357.

17 W. Kläui, A. Müller, W. Eberspach, R. Boese and I. Goldberg, J. Am. Chem. Soc., 109 (1987) 164.

18 E. Dubler, L. Linowsky and W. Kläui, Transition Met. Chem., 4 (1979) 191.

19 (a) A. Bahsoun, J. Dehand, M. Pfeffer, M. Zinsius, S.E. Bouaoud and G. Le Borgne, J. Chem. Soc., Dalton Trans., (1979) 547; (b) M. Pfeffer, J. Fischer and A. Mitschler, Organometallics, 3 (1984) 1531.

20 (a) E.C. Guzman, G. Wilkinson, R.D. Rogers, W.E. Hunter, M.J. Zaworotko and J.L Atwood, J. Chem. Soc., Dalton Trans., (1980) 229; (b) F.A. Cotton and G.A. Rusholme, J. Am. Chem. Soc., 94 (1972) 402.

21 The orientation of the ketenyl group relative to the W(CO){$(CH_3)_3$} part of the molecule is not known.

22 E.O. Fischer, T.L. Lindner and F.R. Kreissl, J. Organomet. Chem., 112 (1976) C27.

23 E. Delgado, J. Hein, J.C. Jeffery, A.L. Ratermann, F.G.A. Stone and L.J. Farrugia, J. Chem. Soc., Dalton Trans., (1987) 1191.

24 International Union of Pure and Applied Chemistry, Commission on Molecular Structure and Spectroscopy, Tables of Wavenumbers for the Calibration of Infra-Red Spectrometers, Butterworths, London, 1961, p. 582.

25 E.O. Fischer and A. Maasböl, Chem. Ber., 100 (1967) 2445.

26 G.A. McDermott, A.M. Dorries and A. Mayr, Organometallics, 6 (1987) 925.

27 Synthesis of trimethylphosphine: W. Wolfsberger and H. Schmidbaur, Syn. React. Inorg. Metal-Org. Chem., 4 (1974), 149; workup procedure: R. Thomas and K. Eriks, Inorg. Synth., 9 (1967) 59.

28 W. Kläui, W. Eberspach and P. Gütlich, Inorg. Chem., 26 (1987) 3977.

29 A.C.T. North, D.C. Phillips and F.S. Mathews, Acta Crystallogr., A, 24 (1968) 351.

30 B.A. Frenz, The Enraf-Nonius CAD4-SDP—A real-time system for concurrent X-ray data collection and crystal structure determination, in: H. Schenk, R. Olthof-Hazekamp, H. van Koningsveld and G.C. Bassi (Eds.), Computing in Crystallography, Delft University Press, Delft, The Netherlands, 1978, pp. 64–71.

31 N. Walker and D. Stuart, Acta Crystallogr., A, 39 (1983) 158.

32 D.T. Cromer and J.T. Waber, International Tables for X-ray Crystallography, Vol. IV, Kynoch Press, Birmingham, 1974, (a) Table 2.2b; (b) Table 2.3.1.